Hindawi
Advances in Mathematical Physics
Volume 2017, Article ID 1016530, 11 pages
https://doi.org/10.1155/2017/1016530

Research Article

Some Discussions about the Error Functions on SO(3) and SE(3) for the Guidance of a UAV Using the Screw Algebra Theory

Yi Zhu, Xin Chen, and Chuntao Li

College of Automation Engineering, Nanjing University of Aeronautics and Astronautics, Nanjing 210016, China

Correspondence should be addressed to Yi Zhu; zhuyi73@126.com

Received 2 August 2016; Revised 3 November 2016; Accepted 29 November 2016; Published 4 January 2017

Academic Editor: Stephen C. Anco

In this paper a new error function designed on 3-dimensional special Euclidean group SE(3) is proposed for the guidance of a UAV (Unmanned Aerial Vehicle). In the beginning, a detailed 6-DOF (Degree of Freedom) aircraft model is formulated including 12 nonlinear differential equations. Secondly the definitions of the adjoint representations are presented to establish the relationships of the Lie groups SO(3) and SE(3) and their Lie algebras so(3) and se(3). After that the general situation of the differential equations with matrices belonging to SO(3) and SE(3) is presented. According to these equations the features of the error function on SO(3) are discussed. Then an error function on SE(3) is devised which creates a new way of error functions constructing. In the simulation a trajectory tracking example is given with a target trajectory being a curve of elliptic cylinder helix. The result shows that a better tracking performance is obtained with the new devised error function.

1. Introduction

The way of computing the tracking errors plays an important role in the guidance process of a UAV. For the problem of either a 2D tracking in a plane or a 3D tracking in the physical space, many valuable researches have been made about the guidance methods of "trajectory tracking" and "path following" [1].

To solve the tracking problems, different researchers hold different opinions. The early methods somewhat originate from the target tracking of missiles such as proportional navigation, way point, and vector field method [2–4]. Then the body-mass point model is usually used so that the direct relationship between the position deviation and speed (or acceleration) can be concerned. Sometimes the influence of the attitude angles and the angular velocity of body frame is also taken into consideration [5]. On the contrary, the features of the inner loops of the aircraft system are often clearly figured out for lager aircrafts [6, 7]. For a 2D tracking issue there are some novel navigation methods and guidance strategies emerging in the light of geometrical intuition and physical interpretation [8–10]. Also, for the curves of 3D trajectories, the constraint of time parameter can be transformed into an arc length parameter by theory of differential geometry [11, 12].

Actually, when a 6-DOF model of an aircraft is concerned, there are at least three basic coordinate frames included which are the inertial frame, the aircraft-body frame, and the airspeed frame. So the coordinate transformations between these different coordinate frames are directly related to the accuracy of the tracking errors computing, that is, where the error functions on SO(3) are used. For examples, in some literatures the guidance strategy is implemented based on a mixed structure of the attitude loops and guidance loops with controllers of the forces and moments [13, 14]. Another instance is the moving frame guidance method. This guidance method changes the ordinary error functions from the inertial frame to a moving frame by orthogonal matrices which belong to SO(3) [15].

Many researches have been made about the formulation of a moving frame of a given trajectory, as recently in [16–19] and previously in [20, 21]. However, the designing of the error functions of a moving frame is a difficulty because there is interdisciplinary knowledge involved such as the Lie group theory. Some literatures indicate that the analyses about the Lie group can be simplified by the screw algebra theory [22].

Theses analyses are important particularly in the tracking process of aircrafts [23, 24]. So in this paper some discussions have been made to provide clear relationships between Lie groups SO(3) and SE(3) and their Lie algebras $so(3)$ and $se(3)$. Then some features of the error functions on SO(3) are proved before a new designed error function on SE(3) is proposed. Thus a new way of error functions constructing is presented. The effects of the different error functions are tested in the simulation with a 6-DOF UAV model.

2. Preliminary

2.1. UAV Model. A flight control system is a bit more complicated than ordinary control systems. The analytic expressions of 6-DOF motion of an aircraft, that is, the 12 nonlinear differential equations, are formulated as follows:

(I) Force equations:

$$\begin{aligned}\dot{u} &= vr - wq - g\sin\theta + \frac{F_x}{m_c},\\ \dot{v} &= -ur + wp + g\cos\theta\sin\phi + \frac{F_y}{m_c},\\ \dot{w} &= uq - vp + g\cos\theta\cos\phi + \frac{F_z}{m_c}.\end{aligned} \tag{1}$$

(II) Kinematic equations:

$$\begin{aligned}\dot{\phi} &= p + \left(q\sin\phi + r\cos\phi\right)\tan\theta,\\ \dot{\theta} &= q\cos\phi - r\sin\phi,\\ \dot{\psi} &= \frac{\left(q\sin\phi + r\cos\phi\right)}{\cos\theta}.\end{aligned} \tag{2}$$

(III) Moment equations:

$$\begin{aligned}\dot{p} &= \left(c_1 r + c_2 p\right)q + c_3\overline{L} + c_4 N,\\ \dot{q} &= c_5 pr - c_6\left(p^2 - r^2\right) + c_7 M,\\ \dot{r} &= \left(c_8 p - c_2 r\right)q + c_4\overline{L} + c_9 N,\end{aligned} \tag{3}$$

where $c_1 = ((I_y - I_z)I_z - I_{xz}^2)/(I_xI_z - I_{xz}^2)$, $c_2 = ((I_x - I_y + I_z)I_{xz})/(I_xI_z - I_{xz}^2)$, $c_3 = I_z/(I_xI_z - I_{xz}^2)$, $c_4 = I_{xz}/(I_xI_z - I_{xz}^2)$, $c_5 = (I_z - I_x)/I_y$, $c_6 = I_{xz}/I_y$, $c_7 = 1/I_y$, $c_8 = (I_x(I_x - I_y) + I_{xz}^2)/(I_xI_z - I_{xz}^2)$, and $c_9 = I_x/(I_xI_z - I_{xz}^2)$.

(IV) Navigation equations:

$$\begin{aligned}\dot{x}_g &= u\cos\theta\cos\psi + v\left(\sin\phi\sin\theta\cos\psi - \cos\phi\sin\psi\right)\\ &\quad + w\left(\sin\phi\sin\psi + \cos\phi\sin\theta\cos\psi\right),\\ \dot{y}_g &= u\cos\theta\sin\psi + v\left(\sin\phi\sin\theta\sin\psi + \cos\phi\cos\psi\right)\\ &\quad + w\left(-\sin\phi\cos\psi + \cos\phi\sin\theta\sin\psi\right),\\ \dot{h}_g &= u\sin\theta - v\sin\phi\cos\theta - w\cos\phi\cos\theta\end{aligned} \tag{4}$$

or

$$\begin{aligned}\dot{x}_g &= V\cos\gamma\cos\varphi,\\ \dot{y}_g &= V\cos\gamma\sin\varphi,\\ \dot{h}_g &= V\sin\gamma,\end{aligned} \tag{5}$$

where m_c is the mass of the aircraft, F_i $(i = x, y, z)$ represents the force of axes of aircraft-body coordinate frame, respectively, $\overline{L}$, M, and N are moments of body frame, u, v, and w are speed components of body frame, θ, ψ, and ϕ represent pitch angle, yaw angle, and bank angle, respectively, p, q, and r are angular velocity from body frame to inertial frame resolved in body frame, x_g, y_g, and h_g represent the position of the aircraft in inertial frame, I_x, I_y, and I_z are rotary inertias of axes of body frame, V is true airspeed, and γ, φ are flight-path angles between the first/second axis of wind coordinate frame and inertial frame, respectively.

In practice, we may not necessarily choose u, v, and w as the state variables of an aircraft model concerning different requirements and we usually choose the true air speed V and aerodynamic angles, such as angle of attack α and sideslip angle β, instead. According to the rotation matrix R_{W2B} from wind frame to body frame, along with the relationship $X_{\text{body}} = R_{W2B}X_{\text{wind}}$, one has the equation

$$\begin{bmatrix}u\\ v\\ w\end{bmatrix} = R_{W2B}\begin{bmatrix}V\\ 0\\ 0\end{bmatrix} = \begin{bmatrix}V\cos\alpha\cos\beta\\ V\sin\beta\\ V\sin\alpha\cos\beta\end{bmatrix}. \tag{6}$$

With (1)~(4) the 12 differential equations are obtained; however it is not adequate to establish a complete nonlinear model of a UAV. More additional parts are needed. Figure 1 shows the inner structure of the UAV dynamic model.

Here δ_e, δ_a, and δ_r are the angular deviations of the elevator, ailerons, and rudder, δ_T is the opening degree of throttle, and Mach represents Mach number. As shown in Figure 1, the actuators are δ_e, δ_a, δ_r, and δ_T rather than forces and moments. Then, it is viable to construct a simulation model of the given aircraft. By (1)~(4) a nonlinear state-space system can be obtained with state variables defined by $\mathbf{X}^T = [u, v, w, \phi, \theta, \psi, p, q, r, x_g, y_g, h]$ and control input vector as $\mathbf{U}^T = [\delta_e, \delta_\alpha, \delta_r, \delta_T]$.

2.2. Adjoint Representations of Lie Algebras. Before the features of the error functions on SO(3) and SE(3) are discussed, the features of SO(3) and SE(3) themselves should be made clear. In the following part, some basic concepts of the screw algebra and Lie group theory are discussed in detail.

According to the screw algebra theory of motions of the rigid body, the definitions and adjoint representations of the 3-dimensional special orthogonal group SO(3), the 3-dimensional special Euclidean group SE(3), and the corresponding Lie algebras $so(3)$ and $se(3)$ are presented as follows.

(I) The 3×3 matrix adjoint representation of $so(3)$ is as follows.

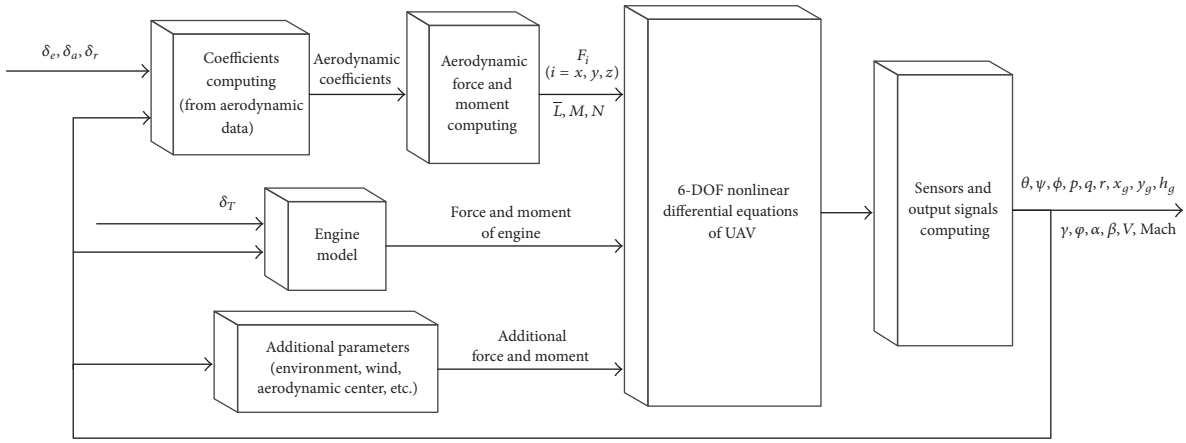

Figure 1: The inner structure of the UAV model.

$so(3)$ is the Lie algebra of the 3-dimensional special orthogonal group SO(3), the adjoint representation of which has a form of a skew-symmetric matrix:

$$\mathrm{ad}(\mathbf{s}) = \mathbf{A}_s = \mathbf{s}^{\wedge} = \begin{bmatrix} 0 & -s_z & s_y \\ s_z & 0 & -s_x \\ -s_y & s_x & 0 \end{bmatrix}. \tag{7}$$

Since the Lie algebra $so(3)$ is represented as a 3×3 skew-symmetric matrix, one basis of the 3-dimensional vector space in the form of matrices is

$$\begin{aligned} \mathrm{ad}(\mathbf{s}_1) &= \mathbf{s}_1^{\wedge} = \begin{bmatrix} 0 & 0 & 0 \\ 0 & 0 & -1 \\ 0 & 1 & 0 \end{bmatrix}, \\ \mathrm{ad}(\mathbf{s}_2) &= \mathbf{s}_2^{\wedge} = \begin{bmatrix} 0 & 0 & 1 \\ 0 & 0 & 0 \\ -1 & 0 & 0 \end{bmatrix}, \\ \mathrm{ad}(\mathbf{s}_3) &= \mathbf{s}_3^{\wedge} = \begin{bmatrix} 0 & -1 & 0 \\ 1 & 0 & 0 \\ 0 & 0 & 0 \end{bmatrix}, \end{aligned} \tag{8}$$

where $\mathbf{s}_1 = (1, 0, 0)^T$, $\mathbf{s}_2 = (0, 1, 0)^T$, and $\mathbf{s}_3 = (0, 0, 1)^T$.

Any elements belonging to $so(3)$ can be represented as a linear combination of this basis.

(II) The standard and adjoint representation of $se(3)$ is as follows.

$se(3)$ is the Lie algebra of the 3-dimensional special Euclidean group SE(3). SE(n), also denoted $\mathrm{E}^+(n)$, is defined to describe rigid body motions including translations and rotations, which is based on an identity of a rigid body motion and a curve in the Euclidean group.

The standard 4×4 matrix representation of $se(3)$ is

$$\mathbf{E} = \begin{bmatrix} \mathbf{s}^{\wedge} & \mathbf{s}_0 \\ \mathbf{0}^T & 0 \end{bmatrix}, \tag{9}$$

where $\mathbf{s}^{\wedge} \in so(3)$ and $\mathbf{s}_0 \in \mathbb{R}^3$. These elements belong to a space which is a subset of $\mathbb{R}^{4\times4}$. The generators of this 6-dimensional vector space are

$$\begin{aligned} \mathbf{E}_1 &= \begin{bmatrix} 0 & 0 & 0 & 0 \\ 0 & 0 & -1 & 0 \\ 0 & 1 & 0 & 0 \\ 0 & 0 & 0 & 0 \end{bmatrix}, \\ \mathbf{E}_2 &= \begin{bmatrix} 0 & 0 & 1 & 0 \\ 0 & 0 & 0 & 0 \\ -1 & 0 & 0 & 0 \\ 0 & 0 & 0 & 0 \end{bmatrix}, \\ \mathbf{E}_3 &= \begin{bmatrix} 0 & -1 & 0 & 0 \\ 1 & 0 & 0 & 0 \\ 0 & 0 & 0 & 0 \\ 0 & 0 & 0 & 0 \end{bmatrix}, \\ \mathbf{E}_4 &= \begin{bmatrix} 0 & 0 & 0 & 1 \\ 0 & 0 & 0 & 0 \\ 0 & 0 & 0 & 0 \\ 0 & 0 & 0 & 0 \end{bmatrix}, \\ \mathbf{E}_5 &= \begin{bmatrix} 0 & 0 & 0 & 0 \\ 0 & 0 & 0 & 1 \\ 0 & 0 & 0 & 0 \\ 0 & 0 & 0 & 0 \end{bmatrix}, \\ \mathbf{E}_6 &= \begin{bmatrix} 0 & 0 & 0 & 0 \\ 0 & 0 & 0 & 0 \\ 0 & 0 & 0 & 1 \\ 0 & 0 & 0 & 0 \end{bmatrix}. \end{aligned} \tag{10}$$

Also there is a 6×6 matrix adjoint representation of $se(3)$ defined as

$$\mathbf{U} = \mathrm{ad}(\mathbf{S}) = \begin{bmatrix} \mathbf{s}^{\wedge} & 0 \\ \mathbf{s}_0^{\wedge} & \mathbf{s}^{\wedge} \end{bmatrix}, \tag{11}$$

where the operator $\mathrm{ad}(\mathbf{S}) \subset \mathbb{R}^{6\times 6}$ is isomorphic to $\mathbf{E}$ and the generators are

$$\begin{aligned} \mathrm{ad}(\mathbf{S}_1) &= \begin{bmatrix} \mathbf{s}_1^{\wedge} & 0 \\ 0 & \mathbf{s}_1^{\wedge} \end{bmatrix}, \\ \mathrm{ad}(\mathbf{S}_2) &= \begin{bmatrix} \mathbf{s}_2^{\wedge} & 0 \\ 0 & \mathbf{s}_2^{\wedge} \end{bmatrix}, \\ \mathrm{ad}(\mathbf{S}_3) &= \begin{bmatrix} \mathbf{s}_3^{\wedge} & 0 \\ 0 & \mathbf{s}_3^{\wedge} \end{bmatrix}, \\ \mathrm{ad}(\mathbf{S}_4) &= \begin{bmatrix} 0 & 0 \\ \mathbf{s}_1^{\wedge} & 0 \end{bmatrix}, \\ \mathrm{ad}(\mathbf{S}_5) &= \begin{bmatrix} 0 & 0 \\ \mathbf{s}_2^{\wedge} & 0 \end{bmatrix}, \\ \mathrm{ad}(\mathbf{S}_6) &= \begin{bmatrix} 0 & 0 \\ \mathbf{s}_3^{\wedge} & 0 \end{bmatrix}. \end{aligned} \tag{12}$$

We can see that the Lie algebra $so(3) \cong \mathbb{R}^3$ is a subspace of $se(3) \cong \mathbb{R}^6$, where the symbol $\cong$ means isomorphic.

(III) The exponential mapping is as follows.

The exponential mapping establishes a connection between $so(3)$ and SO(3), $se(3)$ and SE(3) as well. According to the Rodrigues equation, when the rotation axis $\mathbf{s}$ and the revolute joint θ are given, the rotation matrix $\mathbf{R}$ can be obtained as

$$\mathbf{R} = e^{\theta \mathbf{A}_s} = \mathbf{I} + \sin\theta \mathbf{A}_s + (1 - \cos\theta)\mathbf{A}_s^2, \tag{13}$$

where $\mathbf{s} \in \mathbb{R}^3$, $\mathbf{A}_s = [\mathbf{s}\times] \in so(3)$, and $\mathbf{R} \in \mathrm{SO}(3)$.

Formula (13) presents the exponential mapping from $so(3)$ to SO(3), the proof of which can be found in literature [22].

Similarly, the exponential mapping from $se(3)$ to SE(3) is defined as

$$\mathbf{H} = e^{\theta \mathbf{E}} = e^{\begin{bmatrix} \theta \mathbf{A}_s & \theta \mathbf{s}_0 \\ \mathbf{0}^T & 0 \end{bmatrix}} = \begin{bmatrix} \mathbf{R} & \mathbf{d} \\ \mathbf{0}^T & 1 \end{bmatrix} = \begin{bmatrix} e^{\theta \mathbf{A}_s} & \mathbf{V}\mathbf{s}_0 \\ \mathbf{0}^T & 1 \end{bmatrix}, \tag{14}$$

where $\mathbf{E}$ is the standard 4×4 matrix representation of $se(3)$, and

$$\mathbf{V} = \theta \mathbf{I} + (1 - \cos\theta)\mathbf{A}_s + (\theta - \sin\theta)\mathbf{A}_s^2. \tag{15}$$

(IV) The relationship between SO(3) and SE(3) is as follows.

Special Euclidean group SE(3) is a closed subgroup of 3-dimensional affine group Aff(3). SE(3) can be represented as a semidirect product of the special orthogonal group SO(3) and the translation group $T(3)$; that is,

$$\mathrm{SE}(3) \cong \mathrm{SO}(3) \propto T(3). \tag{16}$$

The geometric meaning of above semidirect product is a rotation motion acting on a translation.

Furthermore, a 6×6 finite displacement screw matrix is defined as

$$\mathbf{N} = \begin{bmatrix} \mathbf{R} & 0 \\ \mathbf{A}\mathbf{R} & \mathbf{R} \end{bmatrix} = \begin{bmatrix} \mathbf{I} & 0 \\ \mathbf{A} & \mathbf{I} \end{bmatrix} \begin{bmatrix} \mathbf{R} & 0 \\ 0 & \mathbf{R} \end{bmatrix} = \mathbf{N}_t \mathbf{N}_r, \tag{17}$$

where rotation matrix $\mathbf{R} \in \mathrm{SO}(3)$ and $\mathbf{A}$ is a skew-symmetric matrix of translation action. Then we can see that

$$\det \mathbf{N} = \det \begin{bmatrix} \mathbf{R} & 0 \\ \mathbf{A}\mathbf{R} & \mathbf{R} \end{bmatrix} = \det \mathbf{R} \det \mathbf{R} = 1. \tag{18}$$

So the finite displacement screw matrix belongs to the special linear group $\mathrm{SL}(n)$, which is a subgroup of the general linear group $\mathrm{GL}(n)$. Also $\mathbf{N}$ is an element of the Lie group SE(3).

3. Error Functions Defined on SO(3) and SE(3)

3.1. General Situation. In the beginning of this section an example is introduced to show the features of equations with matrices belonging to SE(3). The following equations are given:

$$\begin{aligned} \dot{\mathbf{R}} &= \mathbf{R}\boldsymbol{\Omega}^{\wedge}, \\ \dot{\mathbf{P}} &= \mathbf{R}\mathbf{V}, \end{aligned} \tag{19}$$

where $\mathbf{R} \in \mathrm{SO}(3)$ and $\mathbf{P} \in \mathbb{R}^3$. Introduce the matrices $\mathscr{P}$, $\mathscr{G}$ defined by

$$\begin{aligned} \mathscr{P} &= \begin{bmatrix} \mathbf{R} & \mathbf{P} \\ \mathbf{0}_{1\times 3} & 1 \end{bmatrix}, \\ \mathscr{G} &= \begin{bmatrix} \boldsymbol{\Omega}^{\wedge} & \mathbf{V} \\ \mathbf{0}_{1\times 3} & 1 \end{bmatrix}, \end{aligned} \tag{20}$$

where $\mathscr{P} \in \mathrm{SE}(3)$, $\mathscr{G} \in se(3)$ are both 4×4 matrices. The following equation holds:

$$\dot{\mathscr{P}} = \mathscr{P} \cdot \mathscr{G}. \tag{21}$$

Also, there is 6×6 matrix representation of elements of SE(3):

$$\widetilde{\mathscr{G}} = \begin{bmatrix} \boldsymbol{\Omega}^{\wedge} & 0 \\ \mathbf{V}^{\wedge} & \boldsymbol{\Omega}^{\wedge} \end{bmatrix}. \tag{22}$$

These two adjoint representations of 4×4 and 6×6 matrices, that is, $\mathscr{G}$ and $\widetilde{\mathscr{G}}$, are isomorphic to each other. $se(3)$, the Lie algebra of SE(3), is isomorphic to SE(3) as well. It is convenient to choose different forms we need in different situations. However, it is not difficult to verify that the 6×6 matrix representations of SE(3) do not satisfy (21).

This is different from the previous error functions which are defined on SO(3), which is the subgroup of SE(3), such as

$$\Phi\left(\mathbf{R},\mathbf{R}_d\right)=\frac{1}{2}\mathrm{tr}\left[\mathbf{I}-\mathbf{R}_d^T\mathbf{R}\right]. \tag{23}$$

In this paper a trial has been made to define an error function straightforwardly on SE(3), so that the error function will include both the information of the rotation matrix and the position vectors or the speed vectors. The new error function on SE(3) is defined by

$$\Psi\left(\mathbf{R},\mathbf{R}_d,\mathbf{P},\mathbf{P}_d\right)=\frac{1}{2}\mathrm{tr}\left(\left(\mathscr{P}-\mathscr{P}_d\right)^T\mathscr{P}\right). \tag{24}$$

Actually, (24) has a close relationship with $\Phi(\mathbf{R},\mathbf{R}_d)$. Since

$$\begin{aligned}\left(\mathscr{P}-\mathscr{P}_d\right)^T\mathscr{P}&=\begin{bmatrix}\mathbf{R}^T-\mathbf{R}_d^T & \mathbf{0}_{3\times1}\\ \mathbf{P}^T-\mathbf{P}_d^T & 1\end{bmatrix}\begin{bmatrix}\mathbf{R} & \mathbf{P}\\ \mathbf{0}_{1\times3} & 1\end{bmatrix}\\&=\begin{bmatrix}\left(\mathbf{R}^T-\mathbf{R}_d^T\right)\mathbf{R} & \left(\mathbf{R}^T-\mathbf{R}_d^T\right)\mathbf{P}\\ \left(\mathbf{P}^T-\mathbf{P}_d^T\right)\mathbf{R} & \left(\mathbf{P}^T-\mathbf{P}_d^T\right)\mathbf{P}\end{bmatrix},\end{aligned} \tag{25}$$

thus

$$\begin{aligned}\Psi\left(\mathbf{R},\mathbf{R}_d,\mathbf{P},\mathbf{P}_d\right)&=\frac{1}{2}\mathrm{tr}\left(\left(\mathscr{P}-\mathscr{P}_d\right)^T\mathscr{P}\right)\\&=\frac{1}{2}\mathrm{tr}\begin{bmatrix}\mathbf{I}-\mathbf{R}_d^T\mathbf{R} & 0\\ 0 & \|\mathbf{P}\|^2-\mathbf{P}_d^T\mathbf{P}\end{bmatrix}\\&=\frac{1}{2}\mathrm{tr}\left[\mathbf{I}-\mathbf{R}_d^T\mathbf{R}\right]+\frac{1}{2}\left(\|\mathbf{P}\|^2-\mathbf{P}_d^T\mathbf{P}\right).\end{aligned} \tag{26}$$

Hence one can see that with an initial position $\mathbf{P}_0$ and a trajectory $\mathbf{P}_d$, as long as a negative feedback of position signals is guaranteed, the position error $\Delta\mathbf{P}$ is certain to be a decreasing function when it tends to the steady state. So the error function $\|\mathbf{P}\|^2-\mathbf{P}_d^T\mathbf{P}$ is bounded. Let $\mathbf{sup}|\|\mathbf{P}\|^2-\mathbf{P}_d^T\mathbf{P}|=\mathbb{D}$; then the domain of attraction of Ψ is regarded as a linear manifold of Φ. That means some features about the error function Φ defined on SO(3) will still be helpful.

3.2. Error Function on SO(3). To choose the tracking error vectors e_R and e_Ω reasonably, let

$$\overline{\Psi}=\frac{1}{2}\mathrm{tr}\left[\mathbf{I}-\mathbf{R}_d^T\mathbf{R}\right]+\mathbb{D}. \tag{27}$$

By finding the derivative of (27) we have

$$\dot{\overline{\Psi}}=\dot{\Phi}=-\frac{1}{2}\mathrm{tr}\left[\mathbf{R}_d^T\dot{\mathbf{R}}\right]=-\frac{1}{2}\mathrm{tr}\left[\mathbf{R}_d^T\mathbf{R}\Omega^\wedge\right]. \tag{28}$$

Before further discussion, the following properties of 3-order skew-symmetric matrices are presented:

$$\text{(I)}\quad \mathrm{tr}\left(Ax^\wedge\right)=\frac{1}{2}\mathrm{tr}\left[x^\wedge\left(A-A^T\right)\right], \tag{29}$$

$$\text{(II)}\quad \frac{1}{2}\mathrm{tr}\left[x^\wedge\left(A-A^T\right)\right]=-x^T\left(A-A^T\right)^\vee, \tag{30}$$

$$\text{(III)}\quad x\cdot y^\wedge z=y\cdot z^\wedge x,\quad \left(\text{property of the vector mixed product}\right), \tag{31}$$

$$\text{(IV)}\quad x^\wedge y=x\times y=-y\times x=-y^\wedge x, \tag{32}$$

$$\text{(V)}\quad x^\wedge y^\wedge z=x\times\left(y\times z\right)=y\cdot\left(x\cdot z\right)-z\cdot\left(x\cdot y\right)\quad\left(\text{property of the vector triple product}\right), \tag{33}$$

$$\text{(VI)}\quad x^\wedge A+A^Tx^\wedge=\left(\left(\mathrm{tr}\left(A\right)I_{3\times3}-A\right)x\right)^\wedge, \tag{34}$$

$$\text{(VII)}\quad Rx^\wedge R^T=\left(Rx\right)^\wedge, \tag{35}$$

$$\text{(VIII)}\quad \dot{R}-\dot{R}_d\left(R_d^TR\right)=R\left(\Omega-R^TR_d\Omega_d\right)^\wedge. \tag{36}$$

Some proofs of (29)~(36) are clearly given [23, 24]; hence only the proofs of (29), (30), and (36) are given here. First of all, Theorem 1 is presented.

Theorem 1. *Let* $\mathbf{A}$, $\mathbf{B}$ *be* $n\times m$ *and* $m\times n$ *matrices, respectively; then the following equation holds:*

$$\mathrm{tr}\left(\mathbf{AB}\right)=\mathrm{tr}\left(\mathbf{BA}\right). \tag{37}$$

Proof. Let

$$\begin{aligned}\mathbf{A}&=\begin{pmatrix}a_{11} & \cdots & a_{1m}\\ a_{21} & \cdots & a_{2m}\\ \vdots & \ddots & \vdots\\ a_{n1} & \cdots & a_{nm}\end{pmatrix}=\left(a_{ij}\right),\\&\qquad i=1,2,\ldots,n,\ \ j=1,2,\ldots,m,\\ \mathbf{B}&=\begin{pmatrix}b_{11} & \cdots & b_{1n}\\ b_{21} & \cdots & b_{2n}\\ \vdots & \ddots & \vdots\\ b_{m1} & \cdots & b_{mn}\end{pmatrix}=\left(b_{ij}\right),\\&\qquad i=1,2,\ldots,m,\ \ j=1,2,\ldots,n,\end{aligned} \tag{38}$$

and thus

$\mathbf{AB}=(c_{ij})$ is a square matrix of n order, where $c_{ij}=\sum_{k=1}^{m}a_{ik}b_{kj}$, $i,j=1,2,\ldots,n$.

$\mathbf{BA} = (d_{ij})$ is a square matrix of m order, where $d_{ij} = \sum_{k=1}^{n} b_{ik}a_{kj}$, $i, j = 1, 2, \ldots, m$:

$$\begin{aligned}\operatorname{tr}(\mathbf{AB}) &= \sum_{i=1}^{n} c_{ii} = \sum_{i=1}^{n}\sum_{k=1}^{m} a_{ik}b_{ki},\\ \operatorname{tr}(\mathbf{BA}) &= \sum_{i=1}^{m} d_{ii} = \sum_{i=1}^{m}\sum_{k=1}^{n} b_{ik}a_{ki} = \sum_{k=1}^{n}\sum_{i=1}^{m} a_{ki}b_{ik}\\ &= \sum_{i=1}^{n}\sum_{k=1}^{m} a_{ik}b_{ki}.\end{aligned} \tag{39}$$

So tr(**AB**) = tr(**BA**), proof finished. □

In addition, by the definition of the trace of a matrix, for any square matrix **A**, obviously we have

$$\operatorname{tr}(\mathbf{A}) = \operatorname{tr}\left(\mathbf{A}^{T}\right). \tag{40}$$

Then the proof of (29) is presented as follows.

Proof of (29). By (37), (40), and the property of skew-symmetric matrix that

$$-\left(x^{\wedge}\right)^{T} = x^{\wedge}, \tag{41}$$

we have

$$\begin{aligned}\operatorname{tr}\left(Ax^{\wedge}\right) &= \frac{1}{2}\left(\operatorname{tr}\left(x^{\wedge}A\right) + \operatorname{tr}\left(Ax^{\wedge}\right)\right)\\ &= \frac{1}{2}\left(\operatorname{tr}\left(x^{\wedge}A\right) + \operatorname{tr}\left(\left(x^{\wedge}\right)^{T}A^{T}\right)\right)\\ &= \frac{1}{2}\left(\operatorname{tr}\left(x^{\wedge}A\right) + \operatorname{tr}\left(-x^{\wedge}A^{T}\right)\right)\\ &= \frac{1}{2}\left(\operatorname{tr}\left(x^{\wedge}A - x^{\wedge}A^{T}\right)\right)\\ &= \frac{1}{2}\operatorname{tr}\left(x^{\wedge}\left(A - A^{T}\right)\right).\end{aligned} \tag{42}$$

Proof finished. □

Proof of (30). For a three-order square matrix A, it is easy to see that $(A - A^{T})$ is a skew-symmetric matrix. Denoting

$$\begin{aligned}x &= \left[x_1, x_2, x_3\right]^{T},\\ \left(A - A^{T}\right)^{\vee} &= z = \left[z_1, z_2, z_3\right]^{T},\end{aligned} \tag{43}$$

then

$$\begin{aligned}&\frac{1}{2}\operatorname{tr}\left[x^{\wedge}\left(A - A^{T}\right)\right] = \frac{1}{2}\\ &\cdot \operatorname{tr}\left(\begin{bmatrix} 0 & -x_3 & x_2\\ x_3 & 0 & -x_1\\ -x_2 & x_1 & 0\end{bmatrix}\begin{bmatrix} 0 & -z_3 & z_2\\ z_3 & 0 & -z_1\\ -z_2 & z_1 & 0\end{bmatrix}\right)\\ &= \frac{1}{2}\left(\left(-x_2z_2 - x_3z_3\right) + \left(-x_1z_1 - x_3z_3\right)\right.\\ &\left. + \left(-x_1z_1 - x_2z_2\right)\right) = -\left(x_1z_1 + x_2z_2 + x_3z_3\right)\\ &= -x^{T}\left(A - A^{T}\right)^{\vee}.\end{aligned} \tag{44}$$

Proof finished. □

By the definition of the inner product, one has that

$$-x^{T}\left(A - A^{T}\right)^{\vee} = -\left(A - A^{T}\right)^{\vee}\cdot x. \tag{45}$$

By (29), (30), and (45), the following equation holds:

$$\operatorname{tr}\left(Ax^{\wedge}\right) = -\left(A - A^{T}\right)^{\vee}\cdot x. \tag{46}$$

With regard to (46), (28) can be rewritten as

$$\dot{\tilde{\Psi}} = -\frac{1}{2}\operatorname{tr}\left[\mathbf{R}_d^{T}\mathbf{R}\Omega^{\wedge}\right] = \frac{1}{2}\left(R_d^{T}R - R^{T}R_d\right)^{\vee}\Omega, \tag{47}$$

where $(R_d^{T}R - R^{T}R_d) \in so(3)$ is a skew-symmetric matrix, $(\,)^{\vee}$ is the inverse mapping of the hat mapping $(\,)^{\wedge}$. Thus, the tracking error function of attitude can be defined as

$$e_R = \frac{1}{2}\left(R_d^{T}R - R^{T}R_d\right)^{\vee}. \tag{48}$$

Then the proof of (36) is presented as follows.

Proof of (36). According to the rule of finding the derivatives of the rotation matrices with respect to time, we have that

$$\begin{aligned}\dot{R} &= R\Omega^{\wedge},\\ \dot{R}_d &= R_d{\Omega_d}^{\wedge}.\end{aligned} \tag{49}$$

According to (35)

$$\begin{aligned}\dot{R} - \dot{R}_d\left(R_d^{T}R\right) &= R\Omega^{\wedge} - R_d{\Omega_d}^{\wedge}R_d^{T}R\\ &= \left(R\Omega^{\wedge}R^{T} - R_d{\Omega_d}^{\wedge}R_d^{T}\right)R\\ &= \left((R\Omega)^{\wedge} - \left(R_d\Omega_d\right)^{\wedge}\right)R\\ &= \left(R\Omega - R_d\Omega_d\right)^{\wedge}R\\ &= \left(R\left(\Omega - R^{T}R_d\Omega_d\right)\right)^{\wedge}R\\ &= R\left(\Omega - R^{T}R_d\Omega_d\right)^{\wedge}R^{T}R\\ &= R\left(\Omega - R^{T}R_d\Omega_d\right)^{\wedge}.\end{aligned} \tag{50}$$

Proof finished. □

So, we can choose

$$e_\Omega = \Omega - R^T R_d \Omega_d, \tag{51}$$

as the tracking error function of angular velocity vector. Actually, e_Ω is the angular velocity of the rotation matrix $R_d^T R$, which is represented in the body frame, because of the following formulation:

$$\frac{d\left(R_d^T R\right)}{dt} = \left(R_d^T R\right) e_\Omega. \tag{52}$$

The proof of (52) is given as follows.

Proof of (52).

$$\begin{aligned}\frac{d\left(R_d^T R\right)}{dt} &= \frac{d\left(R_d^T\right)}{dt} R + R_d^T \frac{dR}{dt} \\ &= -{\Omega_d}^\wedge R_d^T R + R_d^T R \Omega^\wedge \\ &= R_d^T R \Omega^\wedge - R_d^T R R^T R_d {\Omega_d}^\wedge R_d^T R \\ &= R_d^T R \left(\Omega^\wedge - \left(R^T R_d \Omega_d\right)^\wedge\right) \\ &= R_d^T R \left(\Omega - R^T R_d \Omega_d\right)^\wedge = \left(R_d^T R\right) e_\Omega.\end{aligned} \tag{53}$$

Proof finished. □

In getting the above conclusion the following equations are used:

$$\begin{aligned}\dot{R}_d &= R_d {\Omega_d}^\wedge, \\ \frac{d\left(R_d^T\right)}{dt} &= \left(\dot{R}_d\right)^T = \left(R_d {\Omega_d}^\wedge\right)^T = \left({\Omega_d}^\wedge\right)^T R_d^T \\ &= -{\Omega_d}^\wedge R_d^T.\end{aligned} \tag{54}$$

3.3. Error Function on SE(3). As mentioned above, the error function Ψ is defined as (24) by the 4×4 adjoint matrix representation of elements on SE(3). The benefit of this adjoint representation rests with the simplicity of defining the semidirect product. However, the form of 6×6 matrix representation is adopted here for the convenience of calculation. For a 6×6 matrix $\mathbf{N} \in$ SE(3), according to the principle of Chasles motion decomposition, one has

$$\mathbf{N} = \begin{bmatrix} \mathbf{R} & 0 \\ \mathbf{AR} & \mathbf{R} \end{bmatrix} = \mathbf{N}_l \mathbf{N}_c = \begin{bmatrix} \mathbf{I} & 0 \\ l\mathbf{A}_s & \mathbf{I} \end{bmatrix} \begin{bmatrix} \mathbf{R} & 0 \\ \mathbf{r}_e^\wedge \mathbf{R} & \mathbf{R} \end{bmatrix}, \tag{55}$$

where $\mathbf{R} \in$ SO(3), $\mathbf{A} \in so(3)$, and

$$\mathbf{A} = \mathbf{A}_e + \mathbf{A}_l = \mathbf{A}_e + l\mathbf{A}_s = \mathbf{r}_e^\wedge + l\mathbf{A}_s, \tag{56}$$

l being the Frobenius norm of matrices. By the definition of Frobenius norm, for a matrix $A \in \mathbb{R}^{m \times n}$

$$\|\mathbf{A}\|_F \triangleq \left(\sum_{i=1}^{m} \sum_{j=1}^{n} \left|a_{ij}\right|^2\right)^{1/2} = \left(\mathrm{tr}\left(\mathbf{A}^T \mathbf{A}\right)\right)^{1/2}. \tag{57}$$

For a three-order skew-symmetric matrix $A_x = x^\wedge = \begin{bmatrix} 0 & -x_3 & x_2 \\ x_3 & 0 & -x_1 \\ -x_2 & x_1 & 0 \end{bmatrix}$ which is obtained by a hat mapping, its Frobenius norm is

$$\|\mathbf{A}_x\|_F = \left(2\left(x_1^2 + x_2^2 + x_3^2\right)\right)^{1/2}. \tag{58}$$

Sometimes when it is necessary to change the pitch parameter of a screw and the variable h is added, $\mathbf{N}_h = \begin{bmatrix} \mathbf{I} & 0 \\ h\mathbf{I} & \mathbf{I} \end{bmatrix}$, then

$$\widetilde{\mathbf{N}} = \mathbf{N}_h \mathbf{N} = \begin{bmatrix} \mathbf{I} & 0 \\ h\mathbf{I} & \mathbf{I} \end{bmatrix} \begin{bmatrix} \mathbf{R} & 0 \\ \mathbf{AR} & \mathbf{R} \end{bmatrix} = \begin{bmatrix} \mathbf{R} & 0 \\ \widetilde{\mathbf{A}}\mathbf{R} & \mathbf{R} \end{bmatrix}, \tag{59}$$

where $\widetilde{\mathbf{A}} = h + \mathbf{A}$. See (59) for details and it is can be seen that $\widetilde{\mathbf{N}} \notin$ SE(3) because $\widetilde{\mathbf{A}} \notin so(3)$. Before further discussion of $\widetilde{\mathbf{N}}$, another theorem is presented.

Theorem 2 (the Laplace's expansion theorem). *If k rows (or k columns) of n-order determinant D are selected, where $1 \le k \le n-1$, the sum of products of all the k-order subdeterminants of elements of the k rows (or k columns) and the corresponding algebraic cofactors equals the value of the determinant D.*

Detailed discussions of Laplace's expansion theorem can easily be found in teaching materials of matrix theory or linear algebra, so the proof is omitted here. According to Theorem 2, for a block lower (upper) triangular matrix

$$\mathbf{A} = \begin{bmatrix} \mathbf{B}_{m \times m} & 0 \\ * & \mathbf{C}_{n \times n} \end{bmatrix}, \tag{60}$$

or

$$\mathbf{A} = \begin{bmatrix} \mathbf{B}_{m \times m} & * \\ 0 & \mathbf{C}_{n \times n} \end{bmatrix}, \tag{61}$$

in all the subdeterminants of the first m rows of $\det \mathbf{A}$, only one of them is nonzero. Thus, by expansion of the first m rows, the following deduction is obtained:

$$\det \mathbf{A} = \det(\mathbf{B}) \det(\mathbf{C}). \tag{62}$$

So $\det \widetilde{N} = \begin{bmatrix} \mathbf{R} & 0 \\ \widetilde{\mathbf{A}}\mathbf{R} & \mathbf{R} \end{bmatrix} = \det \mathbf{R} \det \mathbf{R} = 1$, and we can see that $\widetilde{\mathbf{N}} \in$ SL(3) (the special linear group), which is a subgroup of general linear group GL(3).

Similar to (23) and (24), a new error function is defined by

$$\Xi_1 = \mathrm{tr}\left(\mathcal{N}_d^T \mathcal{N} - \mathcal{N}^T \mathcal{N}_d\right), \tag{63}$$

where, with regard to (59), $\mathcal{N}_d = \begin{bmatrix} \mathbf{R}_{H2I} & 0 \\ \widetilde{\mathbf{A}}_H \mathbf{R}_{H2I} & \mathbf{R}_{H2I} \end{bmatrix} \in$ SL(3), $\widetilde{\mathbf{A}}_H = \mathbf{A}_H + h\mathbf{I} = \boldsymbol{\omega}_H^\wedge + h\mathbf{I}$, $\boldsymbol{\omega}_H$ is the Darboux vector of the

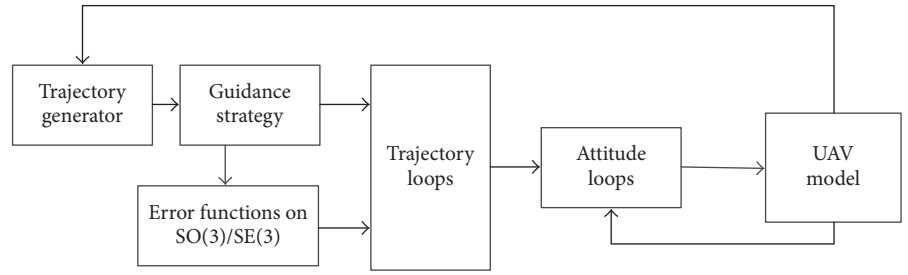

Figure 2: Overview structure of the devised flight control system.

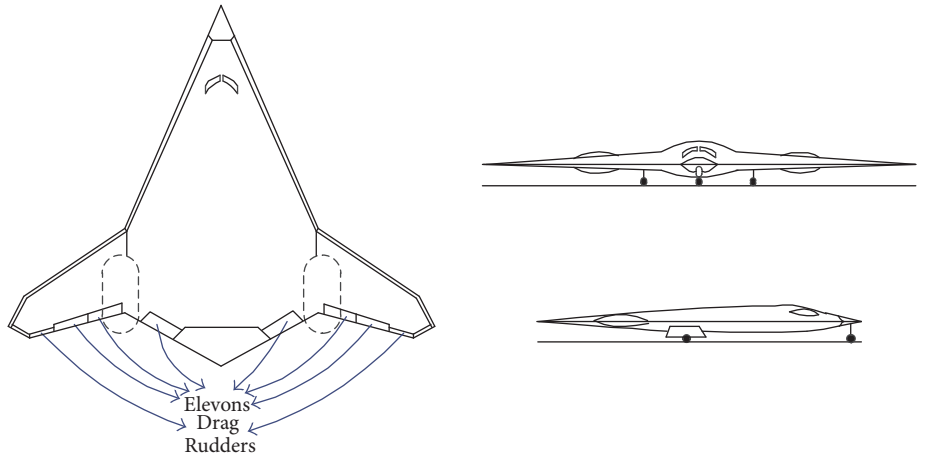

Figure 3: Three-view drawing of the UAV used in the simulations.

frame $\{\mathscr{H}\}$ and $\boldsymbol{\omega}_H^{\wedge} \in so(3)$, $\mathscr{N} = \begin{bmatrix} \mathbf{R}_{B2I} & 0 \\ \mathbf{A}_B\mathbf{R}_{B2I} & \mathbf{R}_{B2I} \end{bmatrix} \in \mathrm{SE}(3)$, and $\mathbf{A}_B = \boldsymbol{\omega}_{\mathrm{Darboux|Bishop}}^{\wedge}$, substituted into (63), and we get

$$\begin{aligned}
\Xi_1 &= \mathrm{tr}\left(\begin{bmatrix} \mathbf{R}_{H2I}^T & \mathbf{R}_{H2I}^T\tilde{\mathbf{A}}_H^T \\ 0 & \mathbf{R}_{H2I}^T \end{bmatrix}\begin{bmatrix} \mathbf{R}_{B2I} & 0 \\ \mathbf{A}_B\mathbf{R}_{B2I} & \mathbf{R}_{B2I} \end{bmatrix}\right. \\
&\quad \left. - \begin{bmatrix} \mathbf{R}_{B2I}^T & \mathbf{R}_{B2I}^T\mathbf{A}_B^T \\ 0 & \mathbf{R}_{B2I}^T \end{bmatrix}\begin{bmatrix} \mathbf{R}_{H2I} & 0 \\ \tilde{\mathbf{A}}_H\mathbf{R}_{H2I} & \mathbf{R}_{H2I} \end{bmatrix}\right) \\
&= \mathrm{tr}\left(\begin{bmatrix} \mathbf{R}_{H2I}^T\mathbf{R}_{B2I} + \mathbf{R}_{H2I}^T\tilde{\mathbf{A}}_H^T\mathbf{A}_B\mathbf{R}_{B2I} & \mathbf{R}_{H2I}^T\tilde{\mathbf{A}}_H^T\mathbf{R}_{B2I} \\ \mathbf{R}_{H2I}^T\mathbf{A}_B\mathbf{R}_{B2I} & \mathbf{R}_{H2I}^T\mathbf{R}_{B2I} \end{bmatrix}\right. \\
&\quad \left. - \begin{bmatrix} \mathbf{R}_{B2I}^T\mathbf{R}_{H2I} + \mathbf{R}_{B2I}^T\mathbf{A}_B^T\tilde{\mathbf{A}}_H\mathbf{R}_{H2I} & \mathbf{R}_{B2I}^T\mathbf{A}_B^T\mathbf{R}_{H2I} \\ \mathbf{R}_{B2I}^T\tilde{\mathbf{A}}_H\mathbf{R}_{H2I} & \mathbf{R}_{B2I}^T\mathbf{R}_{H2I} \end{bmatrix}\right) \\
&= \mathrm{tr}\left(\mathbf{R}_{H2I}^T\mathbf{R}_{B2I} + \mathbf{R}_{H2I}^T\tilde{\mathbf{A}}_H^T\mathbf{A}_B\mathbf{R}_{B2I} - \mathbf{R}_{B2I}^T\mathbf{R}_{H2I}\right. \\
&\quad \left. + \mathbf{R}_{B2I}^T\mathbf{A}_B^T\tilde{\mathbf{A}}_H\mathbf{R}_{H2I} + \mathbf{R}_{H2I}^T\mathbf{R}_{B2I} - \mathbf{R}_{B2I}^T\mathbf{R}_{H2I}\right) \\
&= \mathrm{tr}\left(2\left(\mathbf{R}_{H2I}^T\mathbf{R}_{B2I} - \mathbf{R}_{B2I}^T\mathbf{R}_{H2I}\right)\right. \\
&\quad \left. + \left(\mathbf{R}_{H2I}^T\tilde{\mathbf{A}}_H^T\mathbf{A}_B\mathbf{R}_{B2I} - \mathbf{R}_{B2I}^T\mathbf{A}_B^T\tilde{\mathbf{A}}_H\mathbf{R}_{H2I}\right)\right).
\end{aligned} \tag{64}$$

Let $\mathbf{M}_1 = \mathbf{R}_{H2I}^T\mathbf{R}_{B2I} - \mathbf{R}_{B2I}^T\mathbf{R}_{H2I}$ and $\mathbf{M}_2 = \mathbf{R}_{H2I}^T\tilde{\mathbf{A}}_H^T\mathbf{A}_B\mathbf{R}_{B2I} - \mathbf{R}_{B2I}^T\mathbf{A}_B^T\tilde{\mathbf{A}}_H\mathbf{R}_{H2I}$; then we have $\Xi_1 = \mathrm{tr}(2\mathbf{M}_1 + \mathbf{M}_2)$. Obviously, $\mathbf{M}_1$,$\mathbf{M}_2$ are both skew-symmetric matrices belonging to $so(3)$. Since elements of $so(3)$ have closure property with additive operation, thus $(2\mathbf{M}_1 + \mathbf{M}_2) \in so(3)$. Another vector $\boldsymbol{\omega}_{HB} = \boldsymbol{\omega}_H - \boldsymbol{\omega}_B$ is defined where $\boldsymbol{\omega}_B = \mathbf{A}_B^{\vee} = \boldsymbol{\omega}_{\mathrm{Darboux|Bishop}}$ and another error function is defined by

$$\Xi_2 = \frac{1}{2}\mathrm{tr}\left(\boldsymbol{\omega}_{HB}^{\wedge}\left(2\mathbf{M}_1 + \mathbf{M}_2\right)\right). \tag{65}$$

By (30)

$$\Xi_2 = -\omega_{HB}^T\left(2\mathbf{M}_1 + \mathbf{M}_2\right)^{\vee}. \tag{66}$$

4. Simulations and Analysis

Figure 2 shows an overview structure of the whole flight control system. It is can be seen that there are inner loops (attitude loops and trajectory loops) since the 6-DOF model of the UAV is used. However, the designing of the inner loops is independent of the designing of error functions. So the inner loop controllers are all chosen as ordinary ones.

In the simulations, the employed UAV model originates from an improved and trial type of China's "Sharp Sword" unmanned combat aerial vehicle. Its three-view drawing is shown in Figure 3.

The main data of the UAV are shown in Table 1. From Table 1 it is can be seen that the UAV has a big size of 2300 kg; thus the target trajectory is also a large curve.

Table 1: Data of the UAV in simulations.

Aerodynamic configuration	Flying-wing configuration	Mass of UAV	2.3×10^3 kg
Inertia properties	$I_x = 2.6242 \times 10^3$	Wing span of UAV	8.76 m
	$I_y = 4.5183 \times 10^3$	Max thrust(single engine of two)	500 kgf
	$I_z = 8.9088 \times 10^3$	Max Mach	0.85
	$I_{xy} = I_{zy} = I_{xz} = 0$	Maximum flight altitude	15 km

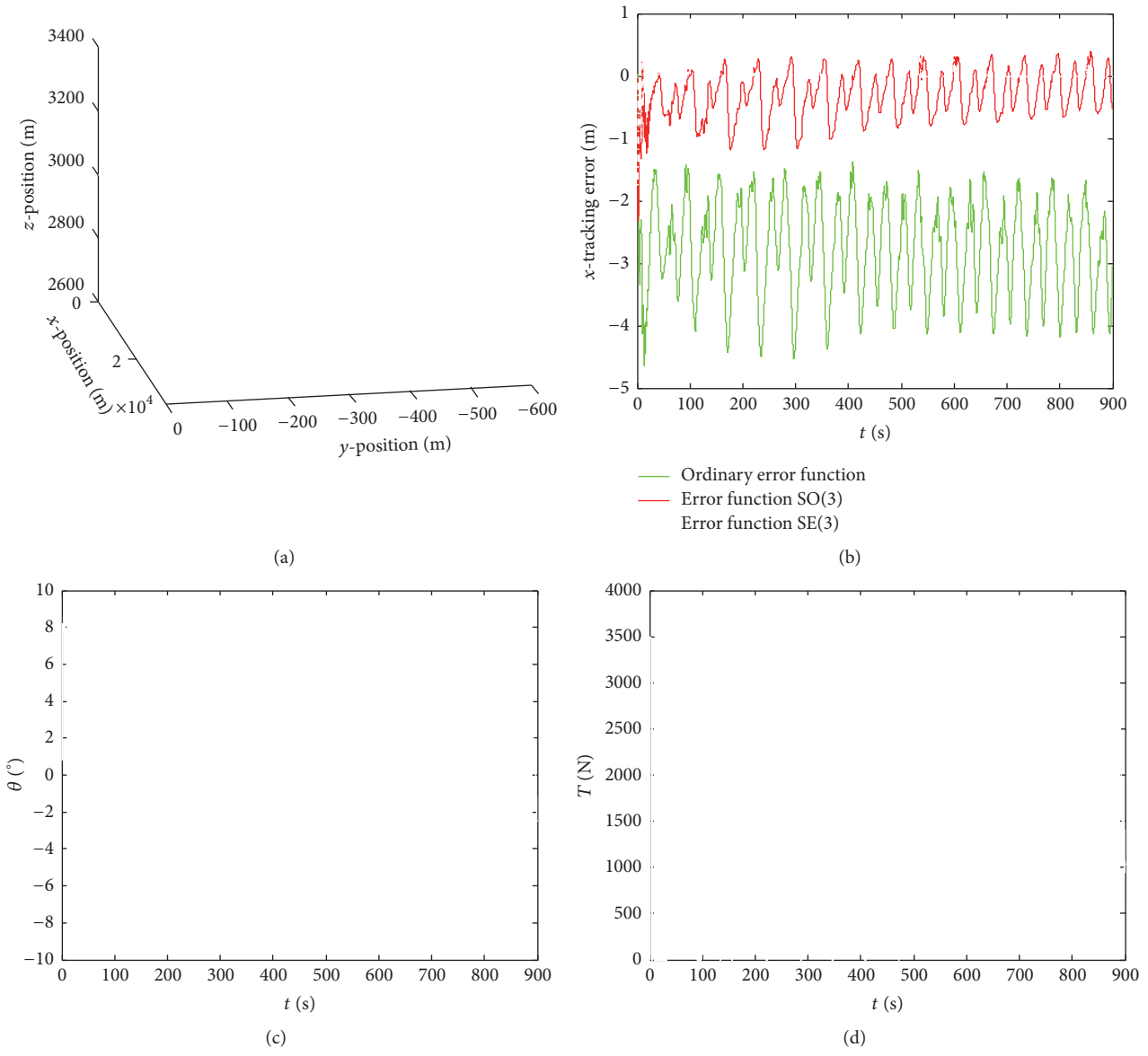

Figure 4: (a) Curve of the target trajectory. (b) A comparison of the forward errors. (c) Curve of the pitch angle. (d) Force of the thrust.

The target trajectory is chosen as an elliptic cylinder helix extending along the horizontal direction. The expression of the given trajectory with regard to a time parameter is defined as

$$\mathbf{r}(t) = \left(a_1 t + c_1, a_2 \cos\left(b_1 t\right) + c_2, a_3 \sin\left(b_2 t\right) + c_3\right)^T, \quad (67)$$

where $a_1, a_2, a_3, b_1, b_2, c_1, c_2, c_3$ are all the coefficients. The beginning of the tracking action is from the moment the UAV arrives in a small neighborhood of any point of the target trajectory. The initial speed vector of body frame is $V_0 = [200, 0, 0]$ and the attitude angles vector is $\phi, \theta, \psi|_0 = [0, 2, 0]$, where the units are, respectively, "m/s" and "∘." According to

the initial condition of the UAV, the values of the coefficients of (67) are finally chosen by

$$\begin{aligned} a_1 &= 200, \\ a_2 &= 300, \\ a_3 &= -250, \\ b_1 &= 0.1, \\ b_2 &= 0.1, \\ c_1 &= 0, \\ c_2 &= -300, \\ c_3 &= -3000. \end{aligned} \tag{68}$$

The curve of the target trajectory $\mathbf{r}(t)$ is shown as in Figure 4(a).

For the similarity of longitudinal and lateral channels of the flight control system, here just take the tracking errors in axis-x for example. In Figure 4(b), the magnitude of tracking error is largest with the ordinary error function. When the error function on SO(3) is added, the tracking error decreases significantly. When the error function on SE(3) is added, the tracking error decreases more. It should be noted that in Figure 4(b) the condition "error function on SE(3)" means "error function on SE(3) is added" so the previous error functions are still being used.

Figure 4(c) shows the tracking curve of the pitch angle θ. The pitch angle is limited in the reasonable ranges with amplitude limits of 20° and 30°. The pitch angle ranges within ±8°. Some slight buffeting near the vertex of the curve of the pitch angle has something to do with the inner loop controllers. Figure 4(d) shows the curve of the single thrust T and there are two engines. In most literatures there is a supposition that the thrust of the aircraft is large enough. Actually a too large thrust means a difficulty in rapid reduction of the forward speed. The UAV mass is about 2300 kg and in simulation the maximum thrust weight ratio is about 0.32. The first 30 s of Figure 4(d) indicates a process of rapid convergence of the forward tracking error. The thrust is controlled directly by the opening degree of the throttle which is constrained in the closed interval $[0, 1]$.

5. Conclusions

According to the nonlinear model of a UAV, a 3D trajectory tracking method is devised. Efforts have been made to discuss the features about the error functions on SO(3) and SE(3). The tracking effect of the flight control system is tested in the numerical simulation. The result of the simulations shows a satisfactory tracking performance so that the error functions designed in this paper are feasible in the UAV tracking process. The designing of the new error function on SE(3) provides a new way of error functions constructing in solving the guidance problem of the UAV.

Competing Interests

The authors declare that there is no conflict of interests regarding the publication of this paper.

References

[1] T. Oliveira, P. Encarnacao, and A. P. Aguiar, "Moving path following for autonomous robotic vehicles," in *Proceedings of the European Control Conference (ECC '13)*, pp. 3320–3325, Zurich, Switzerland, July 2013.

[2] R. Yanushevsky, *Guidance of Unmanned Aerial Vehicles*, CRC Press, 2011.

[3] S. Park, J. Deyst, and J. P. How, "Performance and lyapunov stability of a nonlinear path-following guidance method," *Journal of Guidance, Control, and Dynamics*, vol. 30, no. 6, pp. 1718–1728, 2007.

[4] J. Osborne and R. Rysdyk, "Waypoint guidance for small UAVs in wind," in *Proceedings of the AIAA Infotech Aerospace Conference*, Arlington, Va, USA, September 2005.

[5] H. Chen, K.-C. Chang, and C. S. Agate, "Tracking with UAV using tangent-plus-Lyapunov vector field guidance," in *Proceedings of the 12th International Conference on Information Fusion (FUSION '09)*, pp. 363–372, Seattle, Wash, USA, July 2009.

[6] B. S. Kim, A. J. Calise, and R. J. Sattigeri, "Adaptive, integrated guidance ana control design for line-of-sight based formation flight," in *Proceedings of the AIAA Guidance, Navigation, and Control Conference*, pp. 4950–4972, Keystone, Colorado, August 2006.

[7] A. Matsuura Shinji, "Lateral guidance control of UAV using feedback error learning," in *Proceedings of the AIAA Infotech@Aerospace Conference and Exhibit*, AIAA 2007-2727, Rohnert Park, Calif, USA, May 2007.

[8] S. Park, J. Deyst, and J. How, "A new nonlinear guidance logic for trajectory tracking," in *Proceedings of the AIAA Guidance, Navigation, and Control Conference and Exhibit (AIAA '04)*, Providence, RI, USA, August 2004.

[9] R. Curry, M. Lizarraga, B. Mairs, and G. H. Elkaim, "L^+2, an improved line of sight guidance law for UAVs," in *Proceedings of the 1st American Control Conference (ACC '13)*, pp. 1–6, IEEE, Washington, DC, USA, June 2013.

[10] J. Deyst, J. How, and S. Park, "Lyapunov stability of a nonlinear guidance law for UAVs," in *Proceedings of the AIAA Atmospheric Flight Mechanics Conference 2005*, San Francisco, California, USA, August 2005.

[11] I. Kaminer, O. Yakimenko, A. Pascoal, and R. Ghabcheloo, "Path generation, path following and coordinated control for time-critical missions of multiple UAVs," in *Proceedings of the American Control Conference*, pp. 4906–4913, Minneapolis, Minn, USA, June 2006.

[12] D. Soetanto, L. Lapierre, and A. Pascoal, "Adaptive, Non-Singular Path-Following Control of Dynamic Wheeled Robots," in *Proceedings of the IEEE Conference on Decision and Control*, pp. 1765–1770, Maui, Hawaii, USA, December 2003.

[13] T. Lee, M. Leok, and N. McClamroch, "Geometric tracking control of a quadrotor UAV on SE(3)," in *Proceedings of the 49th IEEE Conference on Decision and Control (CDC '10)*, Atlanta, Ga, USA, December 2010.

[14] V. Cichella, R. Naldi, V. Dobrokhodov, I. Kaminer, and L. Marconi, "On 3D path following control of a ducted-fan UAV on SO(3)," in *Proceedings of the 50th IEEE Conference on Decision*

and Control and European Control Conference (CDC-ECC '11), pp. 3578–3583, Orlando, Fla, USA, December 2011.

[15] V. Cichella, E. Xargay, V. Dobrokhodov, I. Kaminer, A. O. Pascoal, and N. Hovakimyan, "Geometric 3D path-following control for a fixed-wing UAV on SO(3)," in *Proceedings of the AIAA Conference of Guidance, Navigation and Control Conference*, AIAA-2011-6415, Portland, Ore, USA, August 2011.

[16] D. Carroll, E. Köse, and I. Sterling, "Improving Frenet's frame using Bishop's frame," *Journal of Mathematics Research*, vol. 5, no. 4, pp. 97–106, 2013.

[17] S. Kiziltug, S. Kaya, and O. Tarakci, "Tube surfaces with type-2 bishop frame of weingarten types in E^3," *International Journal of Mathematical Analysis*, vol. 7, no. 1–4, pp. 9–18, 2013.

[18] Ş. Kiliçoğlu and H. H. Hacisalihoğlu, "On the ruled surfaces whose frame is the Bishop frame in the Euclidean 3-space," *International Electronic Journal of Geometry*, vol. 6, no. 2, pp. 110–117, 2013.

[19] T. Körpınar and E. Turhan, "Biharmonic curves according to parallel transport frame in E4," *Boletim da Sociedade Paranaense de Matemática*, vol. 31, no. 2, pp. 213–217, 2013.

[20] A. J. Hanson and H. Ma, "Parallel transport approach to curve framing," Tech. Rep., Indiana University Compute Science Department, Bloomington, Ind, USA, 1995.

[21] R. L. Bishop, "There is more than one way to frame a curve," *The American Mathematical Monthly*, vol. 82, pp. 246–251, 1975.

[22] J. S. Dai, *Screw Algebra and Lie Groups and Lie Algebras*, Higher Education Press, Beijing, China, 2014.

[23] T. Lee, "Robust global exponential attitude tracking controls on SO(3)," in *Proceedings of the 1st American Control Conference (ACC '13)*, pp. 2103–2108, Washington, DC, USA, June 2013.

[24] T. Lee, "Geometric tracking control of the attitude dynamics of a rigid body on SO(3)," in *Proceedings of the American Control Conference (ACC '11)*, pp. 1200–1205, San Francisco, Calif, USA, July 2011.